0090-9556/11/3909-1620–1632$25.00
DRUG METABOLISM AND DISPOSITION
Vol. 39, No. 9
36467/3707417
DMD 39:1620–1632, 2011
Printed in U.S.A.

Metabolism of [^{14}C]GSK977779 in Rats and Its Implication with the Observed Covalent Binding

Catherine D. Tsalta, Armina Madatian, Ernest M. Schubert, Fangming Xia, William M. Hardesty, Yanli Deng, Jennifer L. Seymour, and Peter D. Gorycki

Preclinical Drug Metabolism and Pharmacokinetics, GlaxoSmithKline, King of Prussia, Pennsylvania

Received October 24, 2010; accepted May 31, 2011

ABSTRACT:

GSK977779 is a potent HM74a agonist evaluated for the treatment of dyslipidemia. The disposition and metabolism of [^{14}C]GSK977779 (67.6 μmol/kg p.o.) was studied in male and female rats. The compound was well absorbed and its primary route of elimination was in the feces. Based on metabolite profiling of plasma extracts and urine and bile samples, it was demonstrated that GSK977779 was extensively metabolized in the rat by N-dealkylation, mono- and dioxygenation, reductive and oxidative cleavage of the 1,2,4-oxadiazole ring, and conjugative pathways. After plasma extraction high amounts of nonextractable radioactivity were observed, which were more pronounced in female rats. Size-exclusion chromatography and SDS gel electrophoresis indicated that the majority of the nonextractable radioactivity was covalently bound to plasma proteins. Solubilization of the plasma protein pellet followed by high-performance liquid chromatography and mass spectrometry suggested that a carboxylic acid metabolite derived from oxadiazole ring cleavage may be responsible for the observed covalent binding of the radioactivity to rat plasma proteins.

Introduction

GSK977779 is a potent and selective agonist of the HM74a receptor, which was identified as a developmental candidate for the treatment of dyslipidemia. Nicotinic acid (niacin) displays high-affinity binding to HM74a, a seven-transmembrane domain G protein-coupled receptor that has been demonstrated to be responsible for the antilipolytic response to nicotinic acid (Tunaru et al., 2003; Wise et al., 2003; Karpe and Frayn, 2004). Stimulation of the receptor by nicotinic acid or synthetic agonists, such as acipimox or acifran, results in inhibition of adipocyte hormone-sensitive lipase activity and an acute decline in the concentration of nonesterified fatty acids in serum (Fuccella et al., 1980; Grundy et al., 1981). HM74a agonists decrease the plasma levels of triglycerides and low-density lipoprotein cholesterol and increase the plasma levels of high-density lipoprotein cholesterol. Based on head-to-head comparison in nonclinical models, GSK977779 had the potential to be of pharmacologically similar or greater activity than nicotinic acid and to provide a better tolerability profile in humans with respect to flushing.

As part of the nonclinical development program, [^{14}C]GSK977779 (Fig. 1) was administered orally to rats to determine the routes of elimination of the compound and the biotransformation pathways, with emphasis on the identification and quantification of the circulating metabolites. In addition, these studies assessed the extractability of the circulating radioactivity to investigate the potential for covalent binding of GSK977779-related material to plasma proteins. In this manuscript, we describe the main pathways of biotransformation of GSK977779 in the rat and the evaluation of the covalent binding of GSK977779 to rat plasma proteins. The structural elucidation of the metabolites revealed several possibilities for formation of reactive intermediates leading to covalent binding. The experimental methods used for the evaluation of covalent binding, which consisted of solvent extraction, size exclusion chromatography, and SDS-polyacrylamide gel electrophoresis (PAGE), are also described.

Article, publication date, and citation information can be found at http://dmd.aspetjournals.org.
doi:10.1124/dmd.110.036467.

Materials and Methods

Chemicals. [^{14}C]GSK977779D (specific activity 6.52 μCi/mg, radiochemical purity 99.5%) and nonradiolabeled GSK977779 (chemical purity 99.4%) were synthesized and purified by Chemical Development, GlaxoSmithKline Pharmaceuticals (Stevenage, UK). The protein standards (Bio-Rad 161-0324) used for the SDS-PAGE experiments were purchased from Bio-Rad Laboratories (Hercules, CA) and contained the following proteins: myosin (200,000 mol. wt.) β-galactosidase (116,250 mol. wt.), bovine serum albumin (66,000 mol. wt.), ovalbumin (45,000 mol. wt.), carbonic anhydrase (31,000 mol. wt.), soybean trypsin inhibitor (21,500 mol. wt.), lysozyme (14,400 mol. wt.), and aprotinin (6500 mol. wt.). In addition, Laemmli buffer (62.5 mM Tris-HCl, pH 6.8, 2% SDS, 25% glycerol, 0.01% bromophenol blue), Tris-glycine-SDS buffer (25 mM, 192 mM, and 0.1%, respectively, pH 8.3), and 7.5% precast polyacrylamide minigels (10 well, 8.6 × 6.8 cm) were purchased from Bio-Rad Laboratories for the SDS-PAGE experiments. Pooled male or female human liver microsomes and rat liver microsomes were obtained from XenoTech, LLC (Lenexa, KS). All other chemicals and reagents used were of general laboratory grade or better and were purchased from standard commercial sources. Scintillation cocktails Ultima Gold and Ultima Flo M were obtained from PerkinElmer Life and Analytical Sciences (Waltham, MA).

ABBREVIATIONS: PAGE, polyacrylamide gel electrophoresis; BDC, bile duct-cannulated; HPMC, hydroxypropyl methylcellulose; LSC, liquid scintillation counting; HPLC, high-performance liquid chromatography; TCA, trichloroacetic acid; MS, mass spectrometry; LC-MS/MS, liquid chromatography/tandem mass spectrometry; SEC, size-exclusion chromatography; MS^n, multiple stage mass spectrometry.

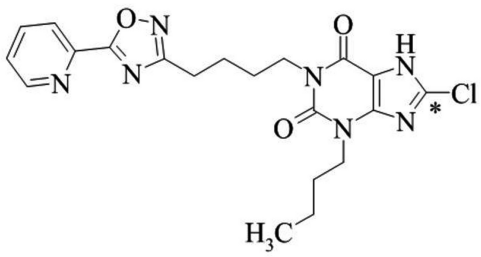

[^{14}C]GSK977779

FIG. 1. Chemical structure of [^{14}C]GSK977779. The asterisk denotes the position of C-14.

Dosing of Animals and Collection of Samples. All of the animal studies were conducted after approval of protocols by the Institutional Animal Care and Use Committee in approved facilities.

Fifteen intact male and 15 intact female Sprague-Dawley rats and three bile duct-cannulated (BDC) male rats (Hilltop Lab Animals, Inc., Scottdale, PA) weighing 250 to 350 g each received a single oral administration of [^{14}C]GSK977779 at a target dose of 30 mg/kg (67.6 μmol/kg) as a suspension in 0.5% (w/v) aqueous hydroxypropyl methylcellulose (HPMC) at 3 mg/ml. Urine and feces were collected from three intact male and three intact female rats predose at different time intervals over 168 h postdose. Urine, bile, and feces were collected from the three BDC rats predose and postdose at various intervals over 96 h postdose. Blood was also collected from three intact animals/sex per time point at 2, 4, 8, and 24 h postdose as terminal bleeds. After a portion of blood had been removed for radioanalysis, the remaining blood was centrifuged to harvest the plasma. Animal cages were rinsed with deionized water after each daily excreta collection. After the last excreta samples were collected, the cages were washed with an ethanol:1% trisodium phosphate solution (1:1; v/v) and wiped with gauze pads. The residual carcasses were retained for bioanalysis. Blood was collected via exsanguination (under isoflurane anesthesia) from selected animals at euthanasia. All postdose samples (bile, urine, feces, blood, plasma, cage rinse, cage wash, residual carcass, and extracts of the bile cannulas, jackets, and cage wipes) were analyzed for total radioactivity.

Additional rats were dosed with [^{14}C]GSK977779 to generate plasma samples for SDS-PAGE experiments. Six male and six female rats obtained from Charles River Laboratories (Wilmington, MA) and weighing 250 to 350 g were administered a single oral dose of either 3 or 30 mg/kg [^{14}C]GSK977779 (three animals/sex per dose group) as a suspension in 0.5% (w/v) aqueous HPMC at 0.3 and 3 mg/ml, respectively. Blood was collected via exsanguination (under isoflurane anesthesia) from each animal at 2, 8, or 24 h postdose (one animal/sex per time point). After a portion of blood had been removed for radioanalysis, the remaining blood was centrifuged to harvest the plasma. An additional two female rats were subsequently dosed with 30 mg/kg nonradiolabeled GSK977779 as a suspension in 0.5% (w/v) aqueous HPMC, and blood was collected from these animals via exsanguination at 24 h postdose. The purpose of this experiment was to obtain plasma, subject it to an exhaustive extraction procedure that involved the precipitation of plasma protein, and analyze the plasma protein to identify any GSK977779-related covalently bound moiety.

Determination of Radioactivity in Plasma, Urine, Bile, Liver, and Feces. Plasma, bile, and urine samples were assayed for radioactivity by liquid scintillation counting (LSC) using Packard TriCarb 3100TR (PerkinElmer Life and Analytical Sciences), and counting efficiency was determined by an external standard ratio procedure. Samples were counted for a preset time of 5 min. When appropriate, samples were dispensed directly into Ultima Gold scintillation cocktail (10 ml). Liver and feces samples were mixed with water at an approximate weight ratio of 1:3. The samples were homogenized using a Polytron 10/35 probe-type homogenizer (Brinkmann Instruments, Westbury, NY), and aliquots weighing 0.2 g each were combusted and analyzed for radioactivity. Combustion was performed with a Packard Oxidizer 307 using Carbosorb E (8 ml; PerkinElmer Life and Analytical Sciences) as the carbon dioxide absorber and Permaflour E+ (12 ml; PerkinElmer Life and Analytical Sciences) as the scintillation cocktail. An aliquot of Combustaid (200 μl; PerkinElmer Life and Analytical Sciences) was added to each sample before combustion. Aliquots of ^{14}C SPEC-CHEC standard (PerkinElmer Life and Analytical Sciences) were combusted throughout the batch to determine oxidizer combustion efficiencies. To convert the radioactivity of sample (disintegrations per minute per gram) to concentration units (microgram equivalent of GSK977779 per gram of sample), a conversion factor of 14.49 dpm/ng was used based on the specific activity of the radiolabel.

Plasma and Liver Sample Preparation for Extractability Determination and Metabolite Profiling. Plasma and liver homogenate samples from individual animals were pooled across each time point using equal volumes (for plasma) or equal weights (for liver) to produce a single representative sample per time point (2, 4, 8, and 24 h). Aliquots of the pooled rat plasma samples were counted by LSC before solvent extraction. Separate aliquots of plasma samples were extracted two times with four volumes of acetonitrile followed by centrifugation. The supernatants from the two extractions were combined and the total extracted radioactivity was determined by LSC. The combined supernatants were evaporated to dryness under nitrogen, reconstituted in 1:1 (v/v) methanol:25 mM ammonium formate, pH 3.5, and analyzed for metabolite profiling by radio-high-performance liquid chromatography (HPLC).

Selected plasma samples that exhibited low extractability in acetonitrile (less than 90% recovery) were extracted exhaustively with 10% (w/v) trichloroacetic acid (TCA) followed by three times extraction with 4:1 (v/v) methanol/diethyl ether. Triplicate aliquots of the TCA extracts and the methanol/ether extracts were radioassayed to determine the percentage recovery of radioactivity in these extracts. The amount of radioactivity recovered from the acetonitrile, TCA, and methanol/ether extractions was reported as total extractable and was expressed as percentage of total sample radioactivity. The same plasma-exhaustive extraction procedure (acetonitrile, followed by TCA and methanol/diethyl ether) was followed for the 24-h plasma generated from two rats dosed with nonradiolabeled GSK977779. The supernatants from this extraction were not used for any further experimentation. Only the plasma protein pellet was analyzed further.

Aliquots of pooled liver homogenate samples were analyzed for radioactivity content before extraction. Separate aliquots (1 g) were then treated with approximately 4 volumes of methanol/water (1:3, v/v), vortex mixed, sonicated for at least 5 min, and rotary mixed for at least 55 min. The samples were then centrifuged at approximately 3100g_{av} using a Beckman AccuSpin FR centrifuge (Beckman Coulter Inc., Fullerton, CA) at ambient temperature for 5 min. The residue was extracted one additional time with the same solvent, and the supernatant was combined with the original extract. The combined extracts were mixed, the total volume was determined, and triplicate aliquots (approximately 0.2 ml) were removed to determine total extracted radioactivity by LSC.

[^{14}C]GSK977779 dosing solution had been added to control rat plasma on the day of dosing. This sample was stored frozen under the same conditions as the other samples until the time of analysis. An aliquot of this spiked control sample was analyzed for total radioactivity by LSC. A separate aliquot was extracted by acetonitrile, and the extract was analyzed by LSC to determine the recovery of radioactivity in the acetonitrile extract.

Solubilization and Analysis of Plasma Protein Pellet. After extraction, the residual plasma protein pellets were incubated with 1 M NaOH (3 ml) at 50°C overnight for solubilization. Triplicate aliquots of the mixtures were removed, neutralized by the addition of an appropriate volume of glacial acetic acid, mixed with 10 ml of scintillation cocktail, and kept at room temperature for approximately 2 h. Samples were then radioassayed by LSC to determine the amount of nonextractable radioactivity in the pellets. Fifty-microliter aliquots of the neutralized mixtures, resulting from the solubilization of the 24-h female and male plasma pellets, were injected onto HPLC for radioprofiling. A 24-h rat plasma pellet generated with nonradiolabeled GSK977779 compound was also incubated with 1 M NaOH (3 ml) at 50°C overnight and subsequently neutralized by an appropriate volume of glacial acetic acid. A 50-μl aliquot of the neutralized mixture was analyzed by HPLC-mass spectrometry (MS) to determine the identity of the released GSK977779-related moiety(ies).

One hundred microliters of unlabeled GSK977779 (1 mM) in 100% acetonitrile was mixed with 900 μl of 1 M NaOH and incubated overnight at 50°C. The solution was neutralized by the addition of an appropriate volume of glacial acetic acid. An aliquot of this solution was analyzed by liquid chro-

matography/tandem mass spectrometry (LC-MS/MS) to check the stability of GSK977779 under these conditions.

Urine and Bile Sample Preparation. A portion of the urine and bile samples was pooled by total weight ratio for each animal to obtain a representative sample accounting for the majority of the excreted radioactivity. Aliquots of urine and bile samples were analyzed by LSC for radioactivity determination. Separate aliquots were centrifuged, and the supernatants were analyzed by LC-MS/MS for quantification and identification of metabolites.

Microsomal Binding Assay. [^{14}C]GSK977779 (10 μM) was incubated with male and female pooled human or rat liver microsomes (0.5 mg of total protein) and 0.1 ml of either an NADPH-generating system or 2% sodium bicarbonate solution in triplicate in a final volume of 0.5 ml of 0.1 M potassium phosphate buffer (pH 7.4) for 0, 30, and 60 min. The NADPH-generating system was freshly prepared in 2% sodium carbonate solution and contained NADP, glucose 6-phosphate, and glucose-6-phosphate dehydrogenase at concentrations of 1.7 mg/ml, 7.8 mg/ml, and 6 units/ml, respectively. Incubations were also conducted in an identical manner with [^{14}C]acetaminophen (10 μM) for 0 and 60 min as a positive control. After termination of the incubations, the reaction mixtures were filtered and the filters were washed five times with 4 ml of methanol/water (90:10, v/v). The filters were then transferred to glass scintillation vials and analyzed for the retained radioactivity by LSC.

GSH Trapping Assay. Two hundred microliters of human liver S9 fractions (2.5 mg/ml), human liver microsomes, or rat liver microsomes, 100 μl of GSH (50 mM) in buffer, and 100 μl of GSK977779 (0.5 mM) or 3-methylindole (the positive control) were incubated in 96-deepwell tubes at 37°C in a water bath. After a 3-min preincubation, the reaction was initiated by adding an NADPH-generating system (100 μl of solution consisting of 2.22 mM NADP, 27.65 mM glucose 6-phosphate, and 6.0 units/ml glucose-6-phosphate dehydrogenase together with 15 mM $MgCl_2$ in 0.1 M phosphate buffer). The final concentrations of the liver in vitro systems and GSK977779 and GSH in the incubation mixture were 1 mg/ml, 100 μM, and 10 mM, respectively. The enzymatic reactions were terminated after 90 min by the addition of 100 μl of acetonitrile containing 6% acetic acid. In parallel, control incubations without the NADPH-generating system, GSH, liver protein matrix, or GSK977779 were conducted. After protein precipitation the samples were centrifuged, and 10 μl of the resulting supernatants were analyzed by ultraperformance liquid chromatography-MS using an Acquity UPLC BEH C18 column (50 $\times$ 2 mm, 1.7 μM; Waters, Milford, MA) and a Sciex API-5000 triple quadrupole mass spectrometer (Applied Biosystems/MDS Sciex, Foster City, CA) with neutral loss scanning of 129 corresponding to the loss of pyroglutamic acid.

Size Exclusion Chromatography. Size exclusion chromatography was performed using Agilent 1100 systems (Agilent Technologies, Santa Clara, CA) similar to those used for radio-HPLC analysis described under *Radio-HPLC Metabolite Profiling*. Aliquots of pooled plasma samples were denatured with two volumes of 6 M guanidine hydrochloride (lot number 15914DE; Sigma-Aldrich, St. Louis, MO) by vortex mixing for 30 s at room temperature. The denatured plasma samples (5–99 μl) were injected onto a BioSep-SEC-S3000 column (300 $\times$ 7.8 mm, 5 μm, pore size 290Å; Phenomenex, Torrance, CA). In addition to the plasma samples, 50 μl of a standard solution containing 0.9 mg/ml albumin (high molecular weight standard) and 0.05 mg/ml GSK977779 (low molecular weight standard) was denatured by mixing with 100 μl of 6 M guanidine HCl, and the mixture was injected onto the BioSep-SEC-S3000 column. HPLC analysis was carried out using an isocratic gradient of 6 M guanidine HCl in water at a flow rate of 0.5 ml/min with a run time of 50 min. For the plasma samples, the fractions were pooled at 0.104 ml per fraction into four 96-well scintillation Luma microtiter plates (PerkinElmer Life and Analytical Sciences). The solvent in the plates was evaporated to dryness at approximately 40°C in an oven. The dried plates were then heat-sealed using Top Seal S film (PerkinElmer Life and Analytical Sciences) and analyzed using a Packard TopCount Scintillation Counter. The resulting TopCount data were imported into Laura software (LabLogic, Tampa, FL) using its LSC import function to construct radiochromatograms. The area under each peak was integrated and expressed as a percentage of the total counts detected. For the albumin and GSK977779 standards, chromatographic run UV detection at 280 nm was used.

SDS Gel Electrophoresis. Plasma samples collected from individual rats administered either 3 or 30 mg/kg [^{14}C]GSK977779 were analyzed by SDS-PAGE. Equal volumes of plasma collected at 2 and 24 h postdose (~10 μl) and Laemmli buffer (Bio-Rad Laboratories) were mixed, and the mixture was heated to 95°C for 3 to 5 min in a stirred water bath. After cooling to room temperature, a 1.5-μl aliquot of the plasma/buffer mixture was loaded per lane onto 7.5% precast PAGE minigels (Bio-Rad Laboratories). Three replicate lanes were created per sample. In addition, a mixture of protein molecular weight standards, treated in the same manner as the plasma samples, was applied on each gel along with the samples. Electrophoresis was performed in a Mini-Protean 3 cell apparatus (Bio-Rad Laboratories) at 200 V, for approximately 35 min using Tris-glycine-SDS (Bio-Rad Laboratories) as the running buffer. The starting current was 50 mA and the ending current was 30 mA. Gels were fixed, stained with Coomassie Blue, destained, and washed. Gel lanes were cut into five sections based on molecular mass: stacking gel, >120, 80 to 120, 20 to 80, and <20 kDa. Gel sections and sample loads were combusted and analyzed by LSC. The radioactivity in each gel section was compared with the amount of radioactivity loaded onto each lane of the gel. The total percentage of radioactivity retained in each lane was calculated by adding the recoveries of individual gel sections.

Radio-HPLC Metabolite Profiling. Radio-HPLC chromatograms were generated on Agilent 1100 systems (Agilent Technologies) equipped with a diode array UV detector and connected to a β-RAM model 2B radiometric detector (LabLogic) with a 500 μl of homogeneous liquid scintillant flow cell and a built in liquid scintillant pump. A Synergi Fusion analytical column (4.6 $\times$ 250 mm, 4-μm particle size; Phenomenex) connected with a guard column (Fusion RP; Phenomenex) was used for metabolite separation. Samples were eluted at a rate of 1 ml/min using a gradient that comprised 25 mM ammonium formate, pH 3.5 (solvent A), and acetonitrile (solvent B). The gradient was as follows: solvent B was held at 12% for the first 5 min and then increased linearly to 27% (5–20 min); it was then held at 27% B from 20 to 35 min, increased linearly to 57% (35–50 min), and then from 50 to 51 min ramped to 95% B and held for 7 min. At 58 to 59 min, the gradient was returned to the initial condition (12% B) for a 9-min isocratic column re-equilibration. Urine and bile samples were analyzed with online radio-detection, during which the eluent was mixed with Ultima Flo M scintillant at a ratio of 1:3 by volume. Radioactivity data were collected at the rate of 1 point/s to plot the radioactive peaks. The percentage of radioactivity in each peak of the metabolic profile was calculated using Laura software (version 3.3.10; LabLogic) and expressed as the percentage of the administered dose recovered in urine and bile corrected for the centrifugation recovery. For plasma extracts that contained insufficient amounts of radioactivity for online radiometric detection, the HPLC eluent was collected into 96-well solid scintillant Luma microtiter plates using a Gilson 222XL liquid handler (Gilson, Inc., Middleton, WI) at 0.150 min/well. The solvent in the microtiter plates was evaporated to dryness at 40°C in an oven (model 1320; VWR Scientific Products, Inc., Plainfield, NJ). The dried plates were then heat-sealed using Top-Seal S film and analyzed using a TopCount NXT scintillation counter (PerkinElmer Life and Analytical Sciences). Each well was counted for 5 min without background subtraction. The resulting TopCount data were imported into the Laura software using its "LSC Import" function and processed by Microsoft Excel 2002 to reconstruct radio-HPLC chromatograms. Each radioactive peak was calculated as a percentage of the total counts detected. The total radioactivity contained in the acetonitrile extracts was also expressed as microgram equivalents of GSK977779 per gram of plasma. The lower limit of quantification was defined as three times the background area integrated in each chromatogram.

Mass Spectrometric Analysis. Metabolite characterization was conducted by one or more of the following: LC-MS^n, LC-multiple reaction monitoring mass spectrometry, and LC-MS accurate mass analysis. The LC conditions were similar to those used for metabolite profiling as described above. HPLC eluent was split at 1:10 ratio between a mass spectrometer and a radiometric flow detector (Packard 515TR; PerkinElmer Life and Analytical Sciences). Nominal mass measurements and MS/MS experiments were performed on a Thermo Fisher LTQ mass spectrometer equipped with an electrospray ionization source (Thermo Fisher Scientific, Waltham, MA). Accurate mass measurements, defined as <5 ppm or <2 mDa from the theoretical mass, were performed on a Waters QToF II equipped with an electrospray ionization source (Waters). All instruments used a CTC PAL autosampler (LEAP Technologies, Carrboro, NC) for sample introduction. Data were acquired and

TABLE 1

Mean recoveries of radioactivity after single oral administration of [^{14}C]GSK977779 (30 mg/kg) to Sprague Dawley rats

Values are the mean ± S.D. (n = 3), where applicable.

	Intact Males	Intact Females	BDC Male
Feces	73.3 ± 1.6	58.3 ± 2.5	19.8 ± 2.4
Urine	19.0 ± 1.2	33.0 ± 3.7	19.1 ± 3.0
Bile	N.A.	N.A.	52.1 ± 4.6
Total[a]	93.3 ± 0.4	93.5 ± 1.6	92.7 ± 0.4

N.A., not applicable.
[a] Includes radioactivity recovered in cage rinse, wash, wipe, and animal carcass.

processed using Xcalibur software (version 1.3; Thermo Fisher Scientific) or Masslynx software (version 3.5; Waters).

Isolation of Metabolites and NMR Analysis. To confirm their structural assignments, metabolites M9, M11, M12, M14, and M5 were isolated from a rat bile sample that was generated through perfusion of a rat liver (procedure not described in this article) and further analyzed by LC-MS/MS and NMR as follows.

An aliquot of the rat bile sample was injected onto an Agilent 1100 system equipped with Phenomenex Synergi Polar RP-80, 250 × 10-mm column connected with a Phenomenex Polar RP, 10 × 10-mm guard column. Metabolites were eluted using a gradient at a flow rate of 4.7 ml/min with solvents A (25 mM ammonium formate, pH 3.5) and B (methanol). The following three-step gradient was used: 30% solvent B (0–10 min), 30 to 80% B (10–110 min) with further increase to 95% B (110–121 min). After elution of GSK977779 and its metabolites, the gradient was switched back to 30% B and the column was thoroughly washed before the next injection. The column eluate containing each of the major radioactive peaks was collected into separate vials. The presence of each metabolite was confirmed by removing an aliquot of the fraction containing the metabolite of interest and analyzed using HPLC-MS. The LC-MS conditions were similar to those described in the above section using positive ionization in full scan mode.

The isolated M9, M11, M12, M14, and M5 samples were further analyzed by NMR spectroscopy for definitive structural assignment. All spectra were obtained on a Bruker Avance DRX 700MHz NMR spectrometer (Bruker BioSpin Corp., Billerica, MA) equipped with a 5-mm TCI CryoProbe (Bruker BioSpin Corp.) maintained at 298 K. Samples were dissolved in a mixture of acetonitrile-d_3 and D_2O (1:1, v/v). ^{1}H and ^{13}C NMR chemical shifts were referenced to the residual solvent signals of acetonitrile (δ_H 1.93 and δ_C 1.3 ppm), as appropriate. All NMR experiments conducted used pulse sequences coded in the standard Bruker software (TopSpin 2.0.4).

Results

Excretion Studies. The mean recoveries of [^{14}C]GSK977779 after single oral administration to rats at a dose of 30 mg/kg (195.6 μCi/kg) are shown in Table 1. The majority of radioactivity was excreted in the feces within 48 h postdose. The fraction of dose excreted by this route was higher in males (73.3%) than in females (58.3%). In contrast, urinary elimination in males (19.0%) was less than that observed in females (33.0%). In BDC animals, 52.1% of the dose was eliminated in the bile while additional 19.1% of the dose was eliminated in the urine. Based on the high percentage of radioactivity recovered in bile and urine of BDC animals (total of 71.2% of dose), it was concluded that [^{14}C]GSK977779 was well absorbed in the rat.

Plasma and Liver Extractability. The concentration of drug-related material in the rat plasma and liver samples expressed as microgram GSK977779 equivalents per gram of sample (micrograms per gram) is presented in Tables 2 and 3, respectively. The recoveries of radioactivity from pooled plasma samples as well as the amount of radioactivity remaining in the plasma pellet after solvent extraction are also shown in Table 2. In male rat plasma, the extractable radioactivity decreased from approximately 87% at 2 h postdose to 56.5% at 24 h. In female rat plasma, the extractable radioactivity was 67% at 2 h and decreased to 6.3% at 24 h postdose. At all time points, the extractable radioactivity was significantly lower in females than in males. The amount of nonextractable radioactivity reached 81.9% of the total plasma radioactivity in females at 24 h postdose. Based on a concentration of 67 mg of protein per gram of rat plasma (Davies and Morris, 1993), the nonextractable radioactivity in the female plasma sample at 24 h corresponded to 1182 pmol of GSK977779 equivalents per milligram of plasma protein. In male and female liver samples, the amount of extractable radioactivity ranged from 85.1% to 98.1%. The lowest extractability was found with the female 24-h liver sample. Based on a concentration of 162 mg of protein per gram of rat liver (Saadane et al., 1996), the nonextractable radioactivity in the female 24-h liver sample corresponded to 18.4 pmol of GSK977779 equivalents per microgram of liver protein.

Microsomal Binding Assay. The NADPH-dependent binding of radioactivity by human or rat male and female liver microsomes was calculated by subtracting the amount of filter-retained radioactivity in the absence of NADPH from the filter-retained radioactivity in the presence of NADPH. The results are shown in Table 4. After 60 min of incubation, the NADPH-dependent binding of [^{14}C]GSK977779-related radioactivity in male and female rat liver microsomes was 177 and 295 pmol/mg protein, respectively, whereas for [^{14}C]acetaminophen it was 75.8 and 22.5 pmol/mg, respectively. In male and female human liver microsomes, the NADPH-dependent binding of [^{14}C]GSK977779-related radioactivity was 136 and 132 pmol/mg protein, respectively, whereas for [^{14}C]acetaminophen it was 104 and 158 pmol/mg, respectively.

TABLE 2

Extractable and nonextractable (bound) radioactivity in plasma samples after single oral administration of [^{14}C]GSK977779 (30 mg/kg) to male and female rats

Time Postdose	Sex	Total Drug-Related Material[a]	%Extractable[b]	%Bound[c]	Bound[d]	%Total Recovery[e]
h		*μg eq/g*			*pmol/mg protein*	
2	M	211	87.3	1.2	83.5	88.5
4	M	157	87.0	2.9	150	89.9
8	M	84	75.2	7.0	195	82.2
24	M	14	56.5	24.8	116	81.3
2	F	226	67.0	18.3	1366	85.3
4	F	149	40.7	43.3	2145	84.0
8	F	90	17.0	75.3	2228	92.3
24	F	44	6.3	81.9	1182	88.2

M, male; F, female.
[a] Mean concentration of radioactivity (n = 3) in plasma of males and females. All other data were obtained from pooled samples per sex across time points.
[b] Percentage of total radioactivity recovered after solvent extraction.
[c] Percentage of total radioactivity recovered after solubilization of the plasma protein pellets.
[d] Bound radioactivity expressed as picomole equivalent of GSK977779 per milligram of plasma protein.
[e] The sum of the percentage extractable and the percentage nonextractable.

TABLE 3

Extractable and nonextractable (bound) radioactivity in liver after single oral administration of [^{14}C]GSK977779 (30 mg/kg) to male and female rats

Time Postdose	Sex	Total Drug-Related Material[a]	%Extractable[b]	%Bound[c]	Bound[d]	%Total Recovery
h		*μg eq/g*			*pmol/mg protein*	
2	M	84.8	97.1	N.A.	N.A.	N.A.
4	M	67.4	98.1	N.A.	N.A.	N.A.
8	M	32.4	97.5	N.A.	N.A.	N.A.
24	M	6.8	90.7	N.A.	N.A.	N.A.
2	F	89.2	97.4	N.A.	N.A.	N.A.
4	F	64.0	95.5	N.A.	N.A.	N.A.
8	F	25.8	88.5	N.A.	N.A.	N.A.
24	F	8.9	85.1	14.9	18.4	100

M, male; F, female; N.A., not applicable.
[a] Mean concentration of radioactivity ($n = 3$) in liver of males and females. Extraction data were obtained from pooled samples per sex across time points.
[b] Percentage of total radioactivity recovered after solvent extraction.
[c] Calculated percentage of total nonextractable (bound) radioactivity assuming a sum of extractable plus nonextractable radioactivity equal to 100% for the female 24-h liver sample. No experimental determination of the bound radioactivity was done for any of the liver samples.
[d] Bound radioactivity expressed as picomole equivalent of GSK977779 per milligram of liver protein.

GSH Trapping Assay. There was no GSH adduct of GSK977779 detected in this experiment. The performance of the positive control for GSH adduct formation (3-methylindole) was consistent with historical data and the literature (Yan et al., 2007).

Size Exclusion Chromatography. Figure 2 shows the UV (280 nm) chromatogram of the albumin and GSK977779 standards after mixing with 6 M guanidine and size-exclusion chromatography. Figure 3 shows a representative size-exclusion radiochromatogram of the guanidine-HCl-treated female, 8-h plasma sample. The radioactivity that eluted in the chromatographic region, where the albumin standard eluted (between 10 and 20 min), was considered to be covalently bound to plasma proteins. The remainder of radioactivity that eluted from the size-exclusion column later than 30 min, in the chromatographic region where small molecules such as GSK977779 elute, corresponded to unbound drug-related material. In male rat plasma, the amount of covalently bound radioactivity increased from 1.2% at 2 h postdose to 30.8% at 24 h postdose (Table 5). In female rat plasma, the percentage of bound radioactivity increased from 23.8% at 2 h to 96.0% at 24 h postdose (Table 5). The SEC results are in good agreement with the extractability data (Table 2) after accounting for the differences in overall recovery of sample radioactivity between the two methods. In addition, by comparison of the percentage bound in Table 2 with the percentage covalently bound in Table 5, it can be concluded that all of the nonextractable radioactivity was covalently bound.

SDS Gel Electrophoresis. Table 6 shows the percentage of plasma radioactivity retained on a polyacrylamide gel after SDS-PAGE of male and female rat samples obtained from single oral dosing of [^{14}C]GSK977779 at 3 and 30 mg/kg. In male rat plasma at 30 mg/kg, the amount of radioactivity retained on the gel increased from 1.3% at 2 h postdose to 24% at 24 h. At the lower dose of 3 mg/kg in male rats, the amount of plasma radioactivity retained on the gel was below the quantification limit of this technique. After a dose of 3 mg/kg, in female rat plasma, the amount of radioactivity retained on the gel was 35% at 2 h and increased to 92% at 24 h postdose. Likewise, at the dose of 30 mg/kg at the 2-h time point, 16% of radioactivity was retained and increased to 78% at 24 h postdose. In all cases, the retained radioactivity was detected primarily in the gel sections where protein standards of 20 to 80 kDa were located, including rat serum albumin (molecular mass, 64.3 kDa; Peters, 1962). By comparison of the percentage bound in Table 2 with the percentage of radioactivity retained on the gel at the dose of 30 mg/kg in Table 6, it can be concluded that nearly 100% of the nonextractable radioactivity was covalently bound to plasma proteins.

Plasma Radioprofiles and Metabolites. Representative radio-HPLC chromatograms of reconstituted plasma extracts, urine and bile samples are depicted in Figs. 4 to 6. Quantification of plasma metabolites based on radio-HPLC is presented in Table 7. Chemical structures of identified [^{14}C]GSK977779 metabolites (including metabolites identified in plasma, urine, or bile samples) are presented in Figs. 7 and 8 and of potential metabolites in Fig. 9. In male rat plasma, the major radiocomponent at all time points was the unchanged parent compound (55–99% of the extractable radioactivity). In female rat plasma, the parent compound was also the predominant radiocomponent at 2, 4, and 8 h postdose, which accounted for 69 to 94% of the extractable radioactivity. At 24 h, the major radiocomponents were M23, which was tentatively identified as a conjugate of an amidine product of the reductive cleavage of the 1,2,4-oxadiazole ring, and a product of dehydrogenation, M35, which accounted for 50 and 24% of the extracted radioactivity, respectively. M14, a metabolite formed by reductive cleavage of the oxadiazole ring and subsequent conversion

TABLE 4

Amount of [^{14}C]GSK977779- or [^{14}C]acetaminophen-related material bound to rat and human liver microsomal protein after incubation in the presence of NADPH

	Binding in the Presence of NADPH			
	Rat		Human	
	pmol/mg			
Incubation time (min)	30	60	30	60
GSK977779 (M)	72.2	177	86.3	136
Acetaminophen[a] control (M)	N.A.	75.8	N.A.	104
GSK977779 (F)	140	295	83.9	132
Acetaminophen[a] control (F)	N.A.	22.5	N.A.	158

M, male; F, female; N.A., not applicable.
[a] Acetaminophen control incubations were performed for 60 min only.

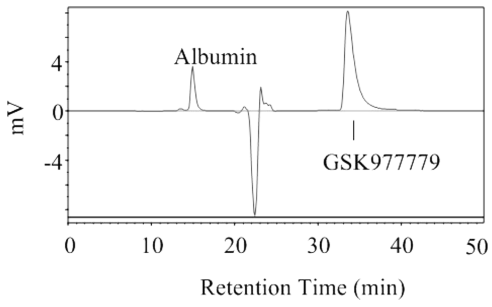

FIG. 2. UV chromatogram of rat serum albumin (0.9 mg/ml) and GSK977779 (0.05 mg/ml) standards at 280 nm after denaturation with 6 M guanidine-HCl and size-exclusion chromatography on a BioSep-SEC-S3000 column.

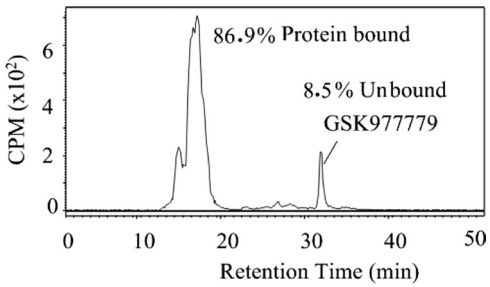

FIG. 3. Representative radiochromatogram of 8-h female rat plasma sample after denaturation with 6 M guanidine-HCl and size-exclusion chromatography on a BioSep-SEC-S3000 column.

to a carboxylic acid, was detected in male and female rat plasma at 2 (only in female) 4, 8, and 24 h postdose and accounted for 1 to 11% of the extracted radioactivity. M4 (amidine), M11 and M12 (products of mono-oxygenation on the *N*-butyl chain), and M21 (another product of mono-oxygenation) were also detected in some male and female plasma samples.

Urine and Bile Radioprofiles and Metabolites. Representative radio-HPLC profiles of pooled rat urine samples after centrifugation are shown in Fig. 5. Quantification of urine metabolites is presented in Table 8. Mass spectrometric analysis allowed for the identification of 76.1, 88.6, and 78.3% of the radioactivity in intact male and female and BDC male urine samples, respectively. In male urine, the predominant metabolite was M9, a product of N-dealkylation, which accounted for 33% of urinary radioactivity (5.8% of dose). Metabolites that resulted from cleavage of the 1,2,4-oxadiazole ring were M14, M4, M31 (mono-oxygenated cleavage product), M26 and M25 (mono-oxygenation plus dehydrogenation products of the amidine derivative), M1 and M2 (mono-oxygenated amidine derivatives), and M34, which together accounted for 35.3% of the urinary radioactivity (6.2% of dose). Additional metabolites were M12, M24, M21, M11 (products of mono-oxygenation), and M17 (product of dioxygenation), which together accounted for 7.8% of the sample radioactivity (1.4% of dose). In pooled female urine, the major metabolites were M4 and M21, which accounted for 21.8 and 26% of the urine radioactivity, respectively (or 6.9 and 8.14% of the dose, respectively). The metabolites that were products of oxadiazole ring cleavage, M4, M14, M34, M31, M25, M26, M2, and M1, accounted for 51.1% of the urinary radioactivity (16.2% of dose). The remainder of the identified

TABLE 5

Unbound and covalently bound radioactivity in plasma samples measured by size exclusion chromatography after single oral administration of [^{14}C]GSK977779 (30 mg/kg) to male and female rats

Time Postdose	Sex	Total Drug-Related Material[a]	%Unbound[b]	%Covalently Bound[c]	Total Recovery[d]
h		*μg eq/g*			
2	M	211	95.7	1.2	96.9
4	M	157	93.8	2.4	96.2
8	M	84.0	87.6	8.5	96.2
24	M	14.0	62.6	30.8	93.4
2	F	226	72.5	23.8	96.3
4	F	149	41.0	55.9	96.9
8	F	90.0	8.5	86.9	95.4
24	F	44.0	2.8	96.0	98.8

M, male; F, female.

[a] Mean concentration of radioactivity ($n = 3$) in plasma of males and females. All other data were obtained from pooled samples per sex across time points.

[b] Amount of radioactivity recovered in chromatographic region where small molecules eluted.

[c] Amount of radioactivity recovered in chromatographic region where albumin standard eluted.

[d] The sum of the percentage unbound and percentage covalently bound radioactivity.

TABLE 6

Amount of radioactivity retained on gel after electrophoresis of plasma samples obtained after single oral administration of [^{14}C]GSK977779 at 3 or 30 mg/kg to male and female rats

Time Postdose (h)	Sex	Total Drug-Related Material (μg/g)		Percentage of Plasma Radioactivity Retained on Gel (Mean ± S.D.)	
		3 mg/kg	30 mg/kg	3 mg/kg	30 mg/kg
2	M	18.0	159	BLQ	1.3 ± 0.1
24	M	1.74	16.2	BLQ	24 ± 4
2	F	10.2	152	35 ± 12	16 ± 3
24	F	2.62	28.4	92 ± 10	78 ± 3

M, male; F, female; BLQ, below the limit of quantification.

metabolites, M21, M12, and M11, accounted for 36.6% of the sample radioactivity (11.5% of dose). An additional metabolite, M32, was detected in female urine by mass spectrometry, but it was not quantifiable by radio-HPLC. This metabolite was a product of oxadiazole ring cleavage plus dioxygenation and dehydrogenation (possibly a carboxylic acid). In both male and female urine, only small amounts of unchanged GSK977779 were detected. The metabolic profile of the BDC male urine was very similar to the profile of the intact male urine sample.

Figure 6 shows the metabolic profile of male BDC rat bile sample. Quantification of biliary metabolites is presented in Table 9. In bile, the metabolites derived from oxadiazole ring cleavage (M4 and M14) accounted for 9.7% of the dose (assuming M4 accounted for the entire radioactivity under the peak where M5 and M17 coeluted). The

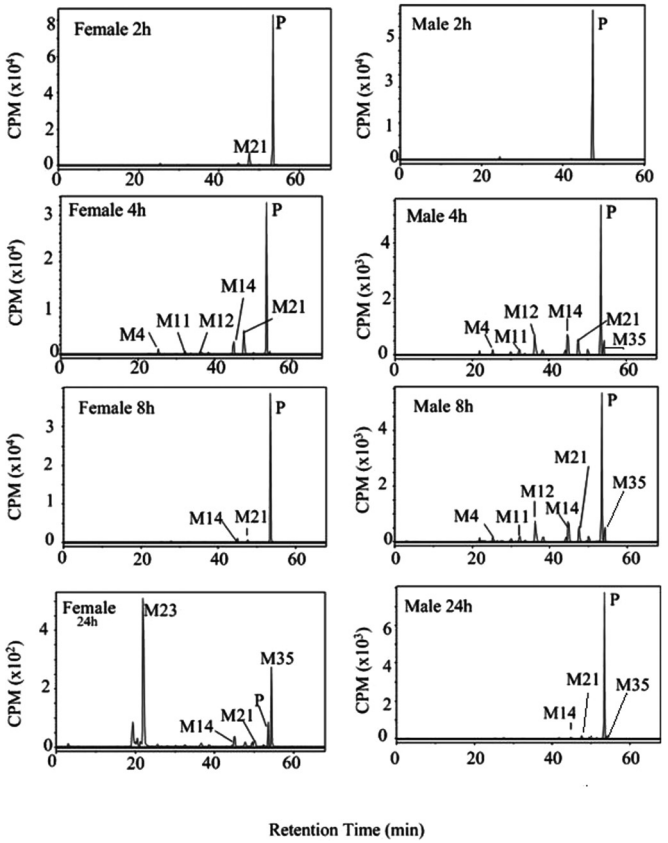

FIG. 4. Representative metabolite radioprofiles of plasma extracts after a single oral administration of [^{14}C]GSK977779 to rats. Metabolite peaks representing less than 2% of the total plasma extract radioactivity are not discernible in this magnification scale of the radiochromatograms. P represents the parent compound. M followed by a number uniquely identifies one metabolite.

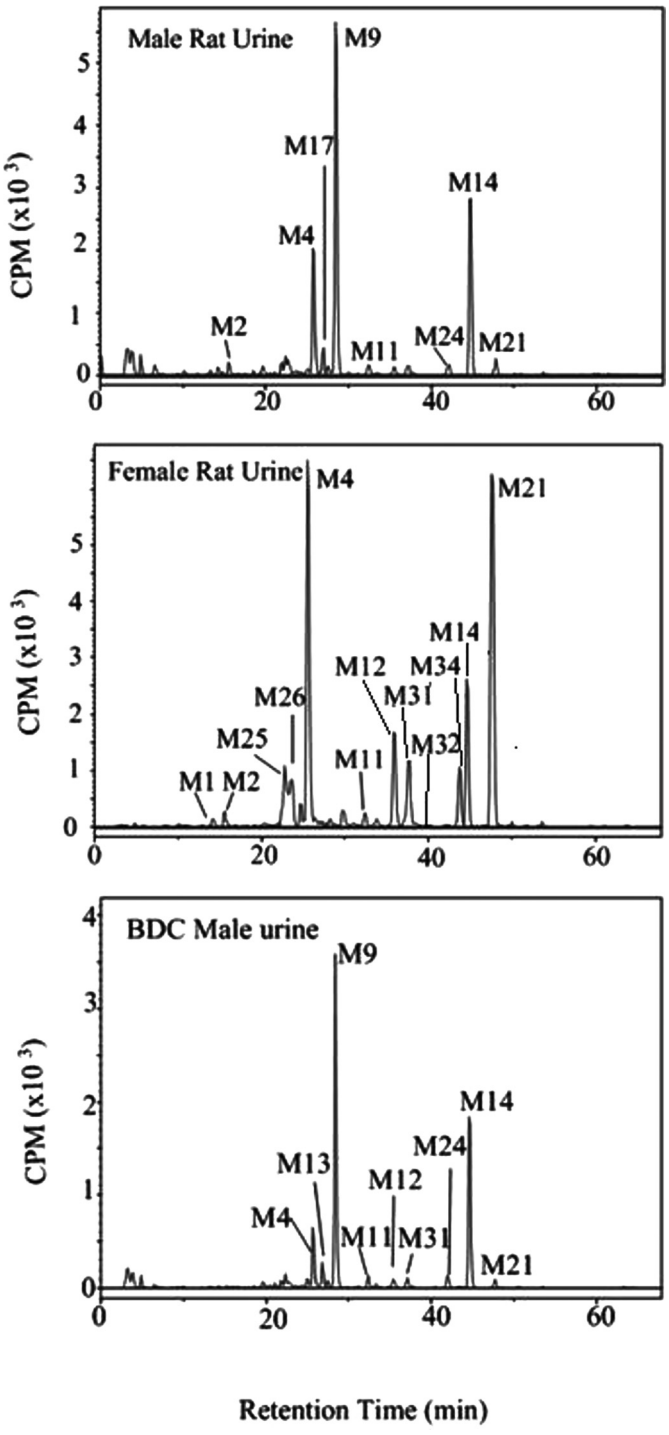

FIG. 5. Representative metabolite radioprofiles of urine samples after a single oral administration of [^{14}C]GSK977779 to rats. P represents the parent compound. M followed by a number uniquely identifies one metabolite.

products of N-dealkylation, mono-oxygenation, and dioxygenation (M9, M12, M21, M11, and M17) together accounted for at least 20.5% of the dose (without including M17, which coeluted with M4 and M5). Additional metabolites identified in bile were as follows: M5, a product of dechlorination, oxidation followed by opening of the fused imidazole ring, and glucuronidation; M10 and M27 (mono-oxygenation plus glucuronidation); M28 (dioxygenation); M29 and M30 (mono-oxygenation plus dechlorination plus GSH conjugation); and M33 (oxidative dechlorination), which together accounted for

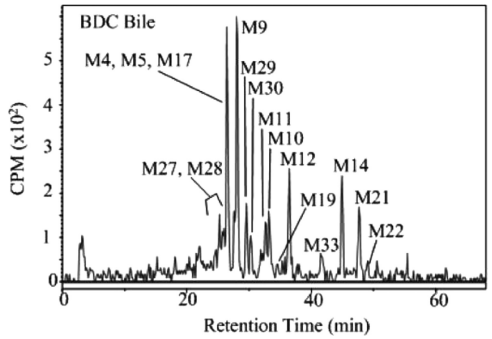

FIG. 6. Representative metabolite radioprofile of bile sample after a single oral administration of [^{14}C]GSK977779 to bile BDC rats. P represents the parent compound. M followed by a number uniquely identifies one metabolite.

approximately 10.6% of the dose. Metabolites M19 and M22 accounted for 0.8 and 0.3% of the dose, respectively, and, based on their mass spectra (Table 10), were identified as a product of dioxygenation plus dehydrogenation and a product of mono-oxygenation, respectively. These minor metabolites with undefined positions of biotransformation were not included in Fig. 7 or Table 9.

Identification of Metabolites by LC-MS/MS and NMR. Metabolite structures were elucidated by LC-MS and NMR analysis. Summaries of LC-MS^n and ^{1}H NMR data are depicted in Tables 10 and 11, respectively. Figure 10 shows the NMR numbering schemes used for GSK977779 and its metabolites. The LC-MS data provided a Markush structure for the metabolites, and further definitive structures on selected metabolites were determined by NMR analysis of isolated metabolites. The MS and NMR structural assignments of the observed circulating metabolites as well as of metabolites M9 and M5 are discussed below. All MS discussion of the pseudo molecular ion and its fragments concern positive $[M + H]^+$ ions, and the reported accurate mass measurements are within 5 ppm or 2 mDa of the theoretical mass.

Metabolite M9. The pseudo molecular ion at *m/z* 388 was 56 Da lower than GSK977779, with accurate mass indicating N-dealkylation. The MS^2 fragments at *m/z* 202 and 187 are assigned to the two ions resulting from the cleavage of the C-N bond located between the xanthine and bridging butyl moieties. Two distinct ^{1}H spin systems were observed in the NMR data. Upon comparison to those observed with GSK977779, these were assigned to the pyridine ring and the butyl chain that links the oxadiazole and xanthine moieties. The notable disappearance of the *n*-butyl ^{1}H NMR signals led to the proposed definitive structure.

TABLE 7

Quantification of radiolabeled metabolites in plasma after single oral administration of [^{14}C]GSK977779 at 30 mg/kg to male and female rats

Parent or Metabolite	Percentage of Total Radioactivity Recovered in Extract[a]							
	Intact Male				Intact Female			
	2 h	4 h	8 h	24 h	2 h	4 h	8 h	24 h
P	98.7	55.7	55.2	94.8	85.7	68.6	93.5	6.36
M4	ND	2.24	1.48	0.26	0.84	2.83	0.57	1.15
M11	ND	3.24	3.20	ND	0.50	1.79	0.38	NQ
M12	ND	12.1	13.2	ND	ND	2.46	0.19	1.15
M14	ND	10.5	10.8	0.80	1.73	7.23	2.67	4.05
M21	1.26	8.85	8.80	2.40	11.2	15.8	1.91	1.73
M23	ND	ND	ND	ND	ND	ND	ND	49.7
M35	ND	7.34	7.30	1.72	ND	1.25	0.76	24.3

P, parent compound; ND, not detected; NQ, detected by mass spectrometry but not quantifiable by radio-HPLC.

[a] Percentage distribution of radioactivity under each identified peak.

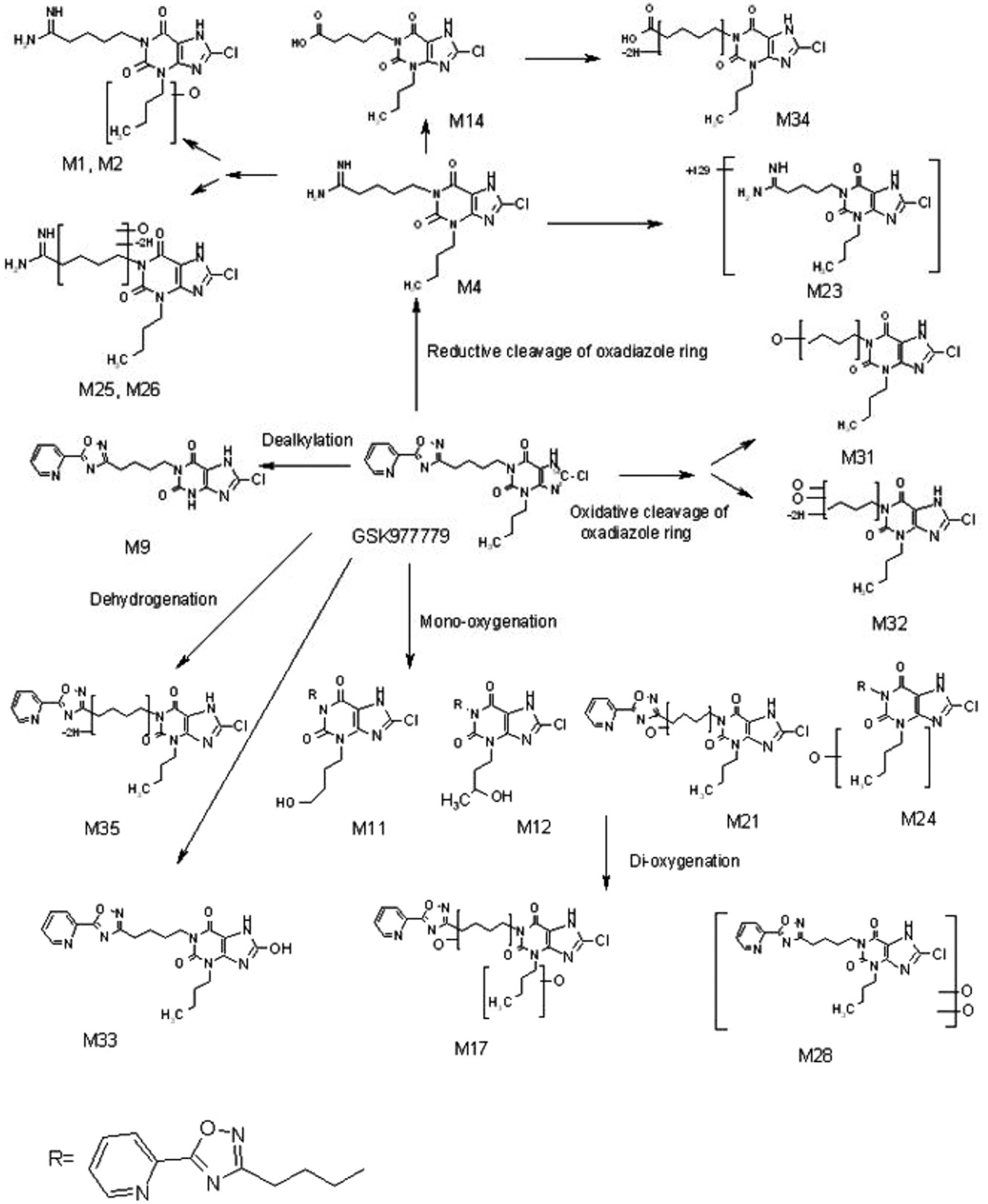

FIG. 7. Proposed Phase I biotransformation pathways of [14C]GSK977779 in rats including an unidentified conjugate detected in plasma. The position of the radiolabel is only shown in the parent compound structure.

Metabolite M11. The pseudo molecular ion at *m/z* 460 was 16 Da higher than GSK977779 with accurate mass indicating mono-oxygenation. MS^2 fragment ions at *m/z* 202 and 187 again show the unchanged oxadiazole pyridine containing the linking butyl chain and chlorinated xanthine moieties, respectively. The fragments at *m/z* 442 and 388 show a loss of water and loss of butanol, respectively, and place the site of biotransformation on the *n*-butyl chain. Three distinct ^{1}H spin systems were observed in the NMR data. Upon comparison to those observed with GSK977779, two of these ^{1}H spin systems may be assigned to the pyridine ring and the butyl chain that links the

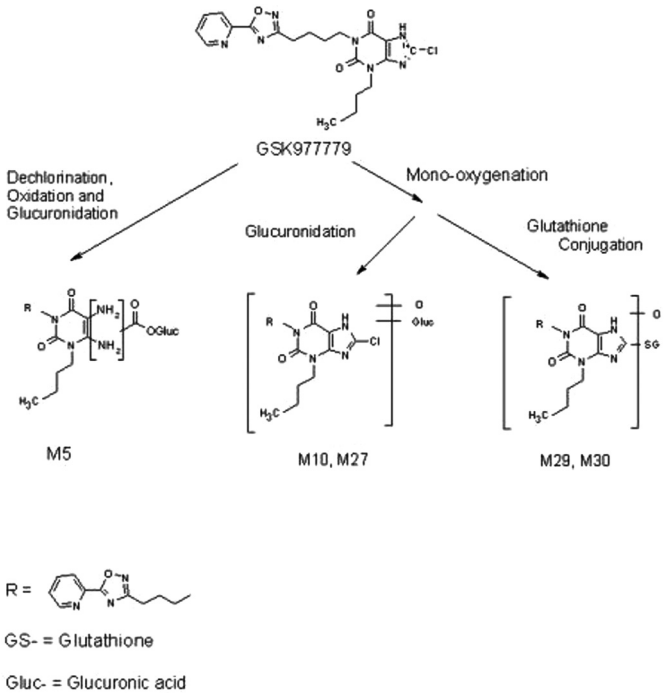

FIG. 8. Phase II metabolites of [^{14}C]GSK977779 detected in rat bile. The position of the radiolabel is only shown in the parent compound structure.

oxadiazole and xanthine moieties. The disappearance of the aliphatic methyl signal in conjunction with the appearance of a new two-proton signal at 3.45 ppm implicate C13 as the site of biotransformation.

Metabolite M12. The observed pseudo molecular ion and MS^2 fragment ions were identical to those observed for metabolite M11, indicating a separate mono-oxygenation of GSK977779 on the same *n*-butyl chain. Likewise, two of the three distinct ^{1}H spin systems observed were assigned to the pyridine ring and the butyl chain that links the oxadiazole and xanthine moieties. The aliphatic methyl signal (shifted downfield 0.25 to 1.06 ppm) was coupled to a CH moiety at 3.68 ppm, identifying C12 as the site of biotransformation.

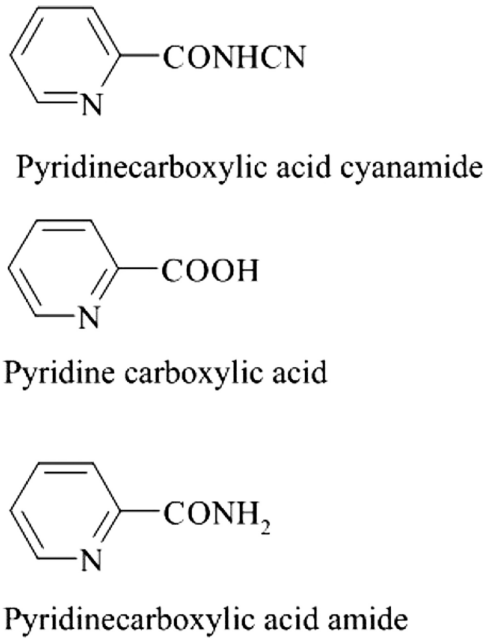

FIG. 9. Putative chemical structures of [^{14}C]GSK977779 metabolites formed by cleavage of the oxadiazole ring but lacking the radiolabel in their structure.

TABLE 8

Quantification of radiolabeled metabolites in urine after single oral administration of [^{14}C]GSK977779 at 30 mg/kg to male and female intact and BDC male rats

Parent or Metabolite Code	Mean Percentage of Urine Radioactivity (Mean Percentage of Administered Dose)[a]		
	Intact Male	Intact Female	BDC male
P	0.04 (0.01)	0.18 (0.05)	ND
M1	1.20 (0.21)	0.39 (0.12)	0.28 (0.05)
M2	0.72 (0.13)	0.74 (0.23)	0.28 (0.05)
M4	12.8 (2.22)	21.8 (6.90)	12.8 (2.11)
M9	33.0 (5.80)	ND	32.9 (5.63)
M11	0.58 (0.10)	0.81 (0.25)	1.12 (0.19)
M12	3.31 (0.58)	9.79 (3.07)	1.35 (0.22)
M14	13.4 (2.37)	8.21 (2.58)	21.1 (3.56)
M17	1.87 (0.33)	0.67 (0.20)	2.23 (0.38)
M21	0.68 (0.12)	26.0 (8.14)	1.35 (0.22)
M24	1.32 (0.24)	ND	1.50 (0.25)
M25	1.38 (0.24)	4.83 (1.55)	0.58 (0.11)
M26	3.36 (0.59)	3.85 (1.22)	1.89 (0.35)
M31	1.91 (0.34)	5.65 (1.80)	0.88 (0.16)
M34	0.51 (0.09)	5.65 (1.76)	ND
Total Quantified[b]	76.1 (13.3)	88.6 (27.9)	78.3 (13.3)

P, parent compound; ND, not detected.
[a] Mean percentage of radioactivity recovered under each peak, also expressed as percentage of the administered dose in parenthesis.
[b] Total quantified represents the percentage of urine sample radioactivity that was assigned structures, also expressed as percentage of the administered dose.

Metabolite M14. The pseudo molecular ion at *m*/*z* 343 was 101 Da lower than GSK977779. The accurate mass MS^2 product ions at *m*/*z* 297 and 243 indicate losses of formic acid and pentanoic acid from the chlorinated xanthine moiety, respectively. Two distinct ^{1}H spin systems were observed in the NMR data. Upon comparison to those observed with GSK977779, these may be assigned to the *n*-butyl side chain and the butyl chain that links the oxadiazole and xanthine moieties. The notable absence of the pyridinyl ring ^{1}H NMR signals led to the proposed definitive structure.

Metabolite M4. The pseudo molecular ion at *m*/*z* 341 was 103 Da lower than GSK977779. Accurate mass of the MS^2 fragment ion *m*/*z* 324 corresponded to the loss of ammonia. Fragments at *m*/*z* 243 and 99 were assigned as ion pairs from the C-N cleavage between the chlorinated xanthine moiety and pentamidine, respectively. The remaining MS^2 fragment ions *m*/*z* 268 and 187 are loss of ammonia plus *N*-butyl dealkylation and dual N-dealkylations of the chlorinated

TABLE 9

Quantification of radiolabeled metabolites in bile after single oral administration of [^{14}C]GSK977779 at 30 mg/kg BDC male rats

Parent or Metabolite Code	Mean Percentage of Bile Radioactivity (Mean Percentage of Administered Dose)
P	0.12 (0.07)
M4, M5, M17[a]	13.6 (6.98)
M9	23.1 (12.0)
M10	4.56 (2.29)
M11	3.61 (1.87)
M12	7.27 (3.71)
M14	5.24 (2.68)
M21	5.56 (2.91)
M27, M28[a]	9.57 (4.91)
M29	2.27 (1.17)
M30	2.19 (1.14)
M33	2.11 (1.08)
Total Quantified	79.2 (40.8)

P, parent compound.
[a] Coelution of metabolites M4, M5, and M17 and metabolites M27 and M28 was observed with the HPLC method used.

TABLE 10

Selected mass spectra data for GSK977779 and its metabolites

Metabolite	*m/z*	
	$[M + H]^+$	Significant MS^2 and MS^3 Product Ions[a]
GSK977779	444	MS^2: 365, 322, 297, 255, 243, 202, 187, 170, 106
M1	357	MS^2: 322, 280, 268, 198, 187, 156, 144
M2	357	MS^2: 322, 280, 268, 198, 187, 156, 144
M4	341	MS^2: 324, 268, 243, 200, 187, 170, 144, 99
M5	620	MS^2: 603, 444, 427
M9	388	MS^2: 266, 202, 199, 187, 170
M10	636	MS^2: 460, 444; MS^3 on 460: 443, 313[b]
M11	460	MS^2: 442, 400, 388, 295, 253, 245, 241, 202, 199, 187
M12	460	MS^2: 442, 400, 388, 295, 253, 245, 241, 202, 199, 187
M14	343	MS^2: 297, 255, 243, 199, 187, 170
M17	476	MS^2: 458; MS^3 on 458: 440, 386, 311, 241, 200, 187[b]
M19	474	MS^2: 456, 428, 309, 245, 212, 202
M21	460	MS^2: 442, 313, 295, 255, 243, 200, 187
M22	460	MS^2: 443, 313, 271, 259, 203, 202, 188, 106
M23	470	MS^2: 425, 324, 130
M24	460	MS^2: 442, 388, 295, 241, 202, 187
M25	355	MS^2: 337; MS^3 on 337: 320, 243, 187, 169, 95[c]
M26	355	MS^2: 337; MS^3 on 337: 320, 243, 187, 169, 95[c]
M27	636	MS^2: 460, 442, 202
M28	476	No MS^n data
M29	731	MS^2: 713, 585, 458, 274, 199, 145
M30	731	MS^2: 713, 585, 458, 274, 199, 145
M31	315	MS^2: 297; MS^3 on 297: 255, 243, 24[b]
M32	329	MS^2: 311; MS^3 on 311: 283, 255, 243, 227, 199, 187, 169[c]
M33	426	MS^2: 304, 279, 248, 237, 225, 202, 169, 123, 106
M34	341	MS^2: 323, 295, 281, 243, 239, 225, 187
M35	442	MS^2: 414, 320, 295, 239, 200, 106

[a] Major or significant positive product ions. Unless otherwise noted, reported MS fragments were acquired on a Waters QToF II.
[b] MS^n data from Thermo Fisher LTQ.
[c] Species exhibited significant in-source fragmentation. The dominant in-source fragment ion ($-H_2O$) is labeled MS^2 and was used to generate additional fragments (MS^3).

xanthine, respectively, indicating one unmodified butyl chain. These fragment ion assignments support the proposed amidine structure shown in Fig. 7.

Metabolite M21. The pseudo molecular ion at *m/z* 460 was 16 Da higher than GSK977779, which indicates mono-oxygenation by accurate mass. The MS^2 fragment ion at *m/z* 442 corresponded to the loss of water. The site of biotransformation was narrowed to the bridging butyl chain from the observation of two key MS^2 product ions: *m/z* 313, which corresponds to the loss of the oxadiazole pyridinyl moiety, and *m/z* 200, which was assigned to the dehydrated butyl oxadiazole pyridinyl moiety. Together, these fragment ions implicate the bridging butyl chain as the source of the observed MS^n water loss.

Metabolite M23. The pseudo molecular ion at *m/z* 470 was 26 Da higher than GSK977779. The MS^2 fragmentation produced only three significant ions (*m/z* 425, 324, and 130) and was insufficient for definitive structural elucidation. However, the observation of the fragment ion at *m/z* 324 suggested that M23 may be a conjugate of metabolite M4 (M4 + 129 Da). The limited number of fragments as well as the low intensity of the fragment ions that limits the mass accuracy, only allow a tentative structural assignment.

Metabolite M35. The pseudo molecular ion at *m/z* 442 was 2 Da lower than GSK977779, indicating a net loss of two protons by accurate mass. The fragment ion at *m/z* 200 is the butyl oxadiazole pyridinyl moiety, and the fragment at *m/z* 295 is the opposing side containing the bridging butyl and xanthine moiety. These accurate mass fragments show a net loss of two protons and narrow the site of biotransformation to the bridging butyl chain.

Metabolite M5. The pseudo molecular ion at *m/z* 620 was 176 Da higher than GSK977779, without the Cl isotope pattern, and had accurate mass indicating glucuronidation. MS^2 fragment ions at *m/z* 603, 444, and 427 correspond to the loss of ammonia, loss of glucuronide, and loss of both, respectively. Four distinct ^{1}H spin systems were observed in the NMR data. Upon comparison to those observed with GSK977779, three of these ^{1}H spin systems may be assigned to the pyridine ring, the butyl chain that links the oxadiazole and xanthine moieties, and the *n*-butyl side chain. The fourth ^{1}H spin system is consistent with the presence of a glucuronic acid moiety. The ^{13}C chemical shift for the anomeric carbon at 103.4 ppm is indicative of an *O*-glucuronide.

Solubilization and Analysis of Plasma Protein Pellet. Figure 11 shows the radioprofile of the alkali hydrolysate of the protein pellet remaining after the extraction of the 24-h female plasma sample. Most of the sample radioactivity eluted as a single radioactive peak at retention time of 44.17 min. Similar results (the same major radiocomponent) were obtained after the solubilization and analysis of the 24-h male plasma protein pellet. The identity of the major radiocomponent was initially assigned based on its HPLC retention time as the carboxylic acid derivative of the 1,2,4-oxadiazole ring cleavage, metabolite M14. After a subsequent experiment that involved dosing of nonradiolabeled GSK977779 to female rats and analysis of the 24-h plasma protein pellet, the identity of the only drug-related component detected in the alkaline hydrolyzate of the pellet was confirmed by LC-MS/MS to be metabolite M14.

GSK977779, when incubated overnight at 50°C with 1 M NaOH in conditions described under *Solubilization and Analysis of Plasma Protein Pellet*, was found to slowly convert to a degradant, which was identified by LC-MS/MS as the *N*-hydroxy derivative of the amidine M4. The estimated amount of GSK977779 which degraded over the course of 19 h was approximately 13% based on comparison of UV peak areas between the degradant and GSK977779 and assuming equal molar absorptivities at 278 nm. The hydrolytic decomposition of the 1,2,4-oxadiazole ring to yield the *N*-hydroxyamidine in the presence of acid or base has been observed earlier by several investigators (Paoloni and Cignitti, 1968; Tyrkov, 2001). This experiment indicated that the oxadiazole ring is relatively stable under the conditions of the pellet solubilization experiment and therefore provided us with some degree of confidence that M14 was not an artifact of the harsh conditions used to solubilize the protein pellet.

TABLE 11

^{1}H NMR data for GSK977779 and selected metabolites[a]

Atom	GSK977779	M5	M9	M11	M12	M14
10	3.88	3.67 and 3.78		3.88	3.92 and 3.96	3.89
11	1.56	1.48		1.62	1.65 and 1.73	1.58
12	1.24	1.18		1.45	3.68	1.26
13	0.81	0.78		3.45	1.06	0.84
14	3.91	3.87	3.87	3.91	3.91	3.84
15	1.63	1.63	1.63	1.63	1.63	1.50
16	1.73	1.74	1.74	1.74	1.74	1.51
17	2.79	2.81	2.80	2.80	2.80	2.18
23	8.12	8.17	8.14	8.13	8.13	
24	8.00	8.02	8.01	8.01	8.01	
25	7.62	7.62	7.62	7.62	7.62	
26	8.68	8.68	8.68	8.68	8.68	
27		4.61				
28		3.37				
29		3.38				
30		3.38				
31		3.53				

[a] Data acquired in 1:1 (v/v) acetonitrile-d_3/D_2O; values are chemical shifts in ppm.

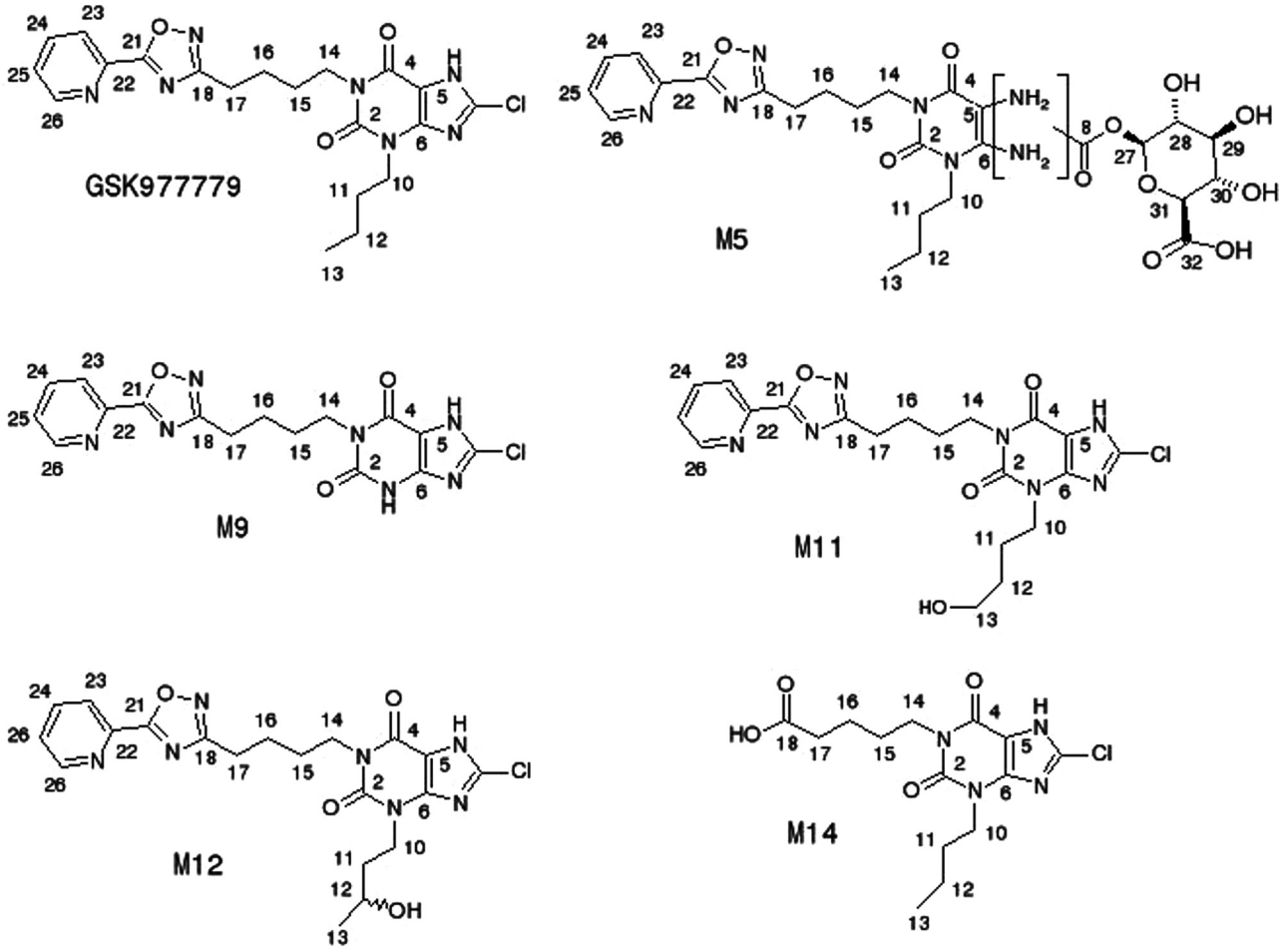

FIG. 10. NMR numbering schemes used for GSK977779 and its metabolites.

Discussion

As indicated by the biliary and urinary metabolic profiles, GSK977779 was extensively metabolized in the rat by the following pathways: N-dealkylation, mono-oxygenation, and dioxygenation; reductive or oxidative cleavage of the oxadiazole ring; and conjugative pathways observed mostly in bile. The metabolic profiles in plasma and urine were qualitatively similar but quantitatively different between male and female rats, as is often the case based on the established gender differences in expression levels of cytochrome P450 and other biotransformation enzymes in this species (Pampori and Shapiro, 1996; Robertson et al., 1998). Overall, the higher metabolism of the parent molecule observed in female rat is consistent with the observation of higher levels of covalent binding in this gender.

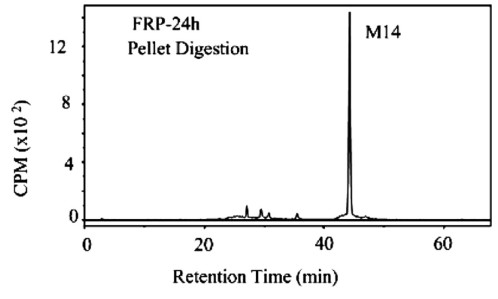

FIG. 11. HPLC radioprofile of the alkali hydrolysate of plasma protein remaining after the extraction of the 24-h female rat plasma sample. The plasma sample was obtained from rats after a single oral dose of [^{14}C]GSK977779 at 30 mg/kg.

During the sample preparation of rat plasma for metabolite profiling, high amounts of nonextractable radioactivity were observed, particularly in female rats. Although there is no absolute threshold over which the concentration of nonextractable radioactivity can be linked with reactive metabolite formation and potential toxicity liabilities, the amount observed with [^{14}C]GSK977779 exceeded by far the tentative threshold of 50 pmol/mg, which has been proposed by other investigators for in vitro or in vivo screening of drug candidates (Evans et al., 2004). Extractability was also measured in male and female rat liver samples and was found to be high relative to plasma. The higher covalent binding observed in plasma may indicate that the main site of bioactivation could be other than the liver (e.g., the intestine) or that the transport properties of the protein complex are favoring the plasma. After incubation of [^{14}C]GSK977779 with rat and human liver microsomes, the amount of NADPH-dependent microsomal protein binding of radioactivity indicated the potential for bioactivation of [^{14}C]GSK977779. In the rat in vitro systems, the NADPH-dependent covalent binding was higher in female than in male, whereas in human liver microsomes there was no significant difference between the two sexes, suggesting that the sex differences could be species specific (Skett, 1988). The observation of high plasma nonextractable radioactivity led to further investigation of the reversibility of the observed binding. SEC and SDS-PAGE have been used in the past to investigate the covalent versus noncovalent binding to plasma proteins (Eling et al., 1977; Zhou et al., 1996; Walsh et al., 2002). SEC and SDS-PAGE of selected plasma samples from rats dosed with [^{14}C]GSK977779 showed that the nonextractable radio-

activity was covalently bound to plasma proteins. Both the cochromatography of radioactivity with the albumin standard in SEC and the appearance of radioactivity primarily in the 20 to 80 kDa gel sections after SDS-PAGE indicated that the bound radioactivity was primarily associated with albumin. The evidence of extensive covalent binding of [^{14}C]GSK977779-related radioactivity suggests that the molecule undergoes bioactivation in rats to one or more reactive metabolites that covalently bind to protein residues. Reactive metabolites are usually short-lived intermediates that are hard to detect in the plasma extracts or in the precipitated plasma protein. However, the identification of the metabolites of the drug-candidate by LC-MS/MS and NMR analysis of plasma and excreta samples may provide indirect evidence regarding the reactive pathway and a basis to propose a mechanism(s) leading to covalent binding. In addition, alkaline hydrolysis of the protein pellet that achieves its solubilization and the release of the bound radioactivity, occasionally allows for the characterization of the structure of the bound metabolite(s) (Bailey and Dickinson, 1996).

It has been reported that the biotransformation of the 1,2,4-oxadiazole can proceed by reductive cleavage to generate amidine, amide, diamide, and carboxylic acid derivatives (Lan et al., 1973; Speed et al., 1994; Ulrich et al., 2001; Bateman et al., 2006). An oxidative cleavage pathway that leads to the formation of a cyanamide has also been reported by Yabuki et al. (1993) and Bateman et al. (2006). In the present report, based on the nature of the identified metabolites, we speculate that the oxadiazole ring is cleaved via both reductive and oxidative mechanisms, with the former being more prominent. Figure 7 shows the proposed Phase I biotransformation pathways of [^{14}C]GSK977779 in rats, including a tentatively identified conjugate of M4 detected in plasma. The metabolites M4, M1, M2, M25, M26, M23, M14, and M34 are products of reductive cleavage, and M31 and M32 are products of oxidative cleavage of the oxadiazole ring. Figure 8 shows the Phase II metabolites of [^{14}C]GSK977779 detected only in rat bile. Complete elucidation of the products of the oxadiazole ring cleavage could not be achieved due to the position of the radiolabel. However, the identification of the cleavage products that retained the radiolabel in their structure allowed us to propose the structure of the metabolites derived from the other half of the molecule. In the case of the oxidative cleavage of the oxadiazole ring, metabolites M32 and M31 provided indirect evidence for the formation of the pyridinecarboxylic acid cyanamide. Other putative products of the reductive cleavage of GSK977779 are the pyridinecarboxylic acid or the pyridine carboxylic acid amide. Figure 9 displays the structures of the three putative metabolites.

Oxadiazole ring metabolism has been studied by many investigators; however, to our knowledge, its implication with covalent binding has not been documented in the literature before. Oxamide resulting from cleavage of oxadiazole ring has been reported to be responsible for long-lived radioactivity in dog plasma, but, according to the authors, there was no evidence for covalent binding of oxamide to plasma protein (Allan et al., 2006). In the case of GSK977779, several metabolite structures raised reactive metabolite alerts, including the products of the reductive cleavage of the oxadiazole ring (the amidine, M4, and its mono-oxygenated derivatives, M1 and M2; metabolites M25 and M26, the unidentified conjugate M23, and the carboxylic acid, M14), the product of oxadiazole ring cleavage and dehydrogenation M34, metabolite M32 (possibly deriving from oxidative cleavage of the oxadiazole and carboxylic acid formation), the GSH conjugates (M29 and M30), and metabolite M5, an acyl glucuronide. The detection of M4, M23, and the other amidine derivatives suggested that the amidine group could potentially form a conjugate with a carboxyl group from a macromolecule. Amidine groups can form noncovalent, hydrogen bonds with carboxyl groups of macromolecules (Peters et al., 2001). Such bonds should be disrupted by treatment with 6 M guanidine hydrochloride (Peters et al., 2001). Our SEC experiments showed that the [^{14}C]GSK977779-related radioactivity remained bound to protein even after 6 M guanidine treatment, suggesting the irreversible nature of the binding through a mechanism other than an amidine-carboxylic acid hydrogen bond. Covalent binding could also occur from the addition of a cysteine group of a macromolecule on an alkene intermediate in a Michael fashion. This type of reaction is usually observed in the presence of an electron withdrawing group adjacent to the double bond (Kalgutkar and Soglia, 2005). Such an example exists for M34, which may contain a double bond at a α-position to the carboxyl group. The results of the in vitro GSH trapping experiment, where no GSK977779-related GSH adduct was detected, indicated that the addition of a cysteine group of a macromolecule to an alkene containing metabolite of GSK977779 was not the likely pathway leading to covalent binding with this molecule. In vivo, the GSH conjugates M29 and M30, which were detected at low levels in rat bile, were products of nucleophilic substitution of the chlorine atom. Indirect evidence that this pathway was not the predominant pathway leading to covalent binding was provided from in vivo experiments with another molecule, compound BA, with structural similarities to GSK977779 (Fig. 12). This compound that contained the same substituted purine ring and differed from GSK977779 only in the composition of the R group (left part of the molecule) did not demonstrate any covalent binding after dosing to rats.

To release the covalently bound moiety of GSK977779, the precipitated protein samples from the 24-h male and female plasma were treated with alkali to hydrolyze the amino acid backbone and potentially the covalent bond with the drug. The chromatographic analysis of the solubilized protein yielded one major peak that was identified as metabolite M14. It is possible that the harsh alkali treatment of the protein pellet had altered the structure of the bound metabolite.

Overall, based on the above experiments, we cannot claim that we positively identified the covalently bound moiety to plasma protein. However, the results of the GSH trapping assay as well as the abolishment of covalent binding by replacement of the oxadiazole ring in compound BA suggested that one or more products of the oxadiazole ring cleavage resulted in the observed covalent binding with GSK977779. In addition, the analysis of the solubilized plasma protein pellet further suggested the possibility that the bound moiety could be the carboxylic acid M14 or a derivative thereof. A number of carboxylic acids have been associated with adverse reactions linked to the metabolic activation through formation of acyl glucuronides or acyl-CoA esters (Skonberg et al., 2008). In the case of GSK977779, covalent binding could have resulted from further bioactivation of M14 by formation of an acyl glucuronide or an acyl-CoA ester.

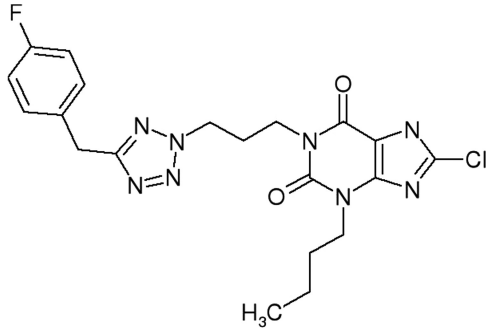

FIG. 12. Chemical structure of compound BA.

However, such metabolites have not been detected in rat plasma or other matrices, possibly due to their high reactivity.

The finding of extensive covalent binding of drug-related material to plasma or liver protein following compound administration to preclinical species constitutes an alert for the potential for idiosyncratic toxicity that, together with other factors such as the anticipated clinical dose level, duration of the treatment, and severity of the therapeutic indication should guide the risk assessment for the drug candidate. In the case of GSK977779, the molecule initially did not raise any structural alerts, was found to be nongenotoxic based on in vitro and in vivo genotoxicity testing, and was well tolerated in a 7-day repeat dose toxicity study in the rat. However, the finding of extensive covalent binding in rats contributed to the termination of this candidate from progression to human trials. Further investigations regarding the identity of the covalently bound metabolite could be performed using enzyme digestion of the isolated protein adduct or matrix-assisted laser desorption/ionization MS to analyze the plasma protein-GSK977779-related adduct. This research would be of broad interest to the pharmaceutical community because the oxadiazole ring is commonly used in place of ester linkages in the structures of xenobiotics (Watjen et al., 1989).

Acknowledgments

We thank Drs. Cosette Serabjit-Singh, Gary Bowers, Giovanni Vitulli, Kitaw Negash, Tom Wilde, Hermes Licea-Perez, Steve Castellino, and David Wagner; and Jill Pirhalla, Caroline Sychterz, Mike Morris, Laura Fotiou, and John Ulicne for their scientific input and assistance in the preparation of the manuscript.

Authorship Contributions

Participated in research design: Tsalta, Madatian, Deng, Seymour, and Gorycki.

Conducted experiments: Madatian, Schubert, Xia, Deng, and Seymour.

Performed data analysis: Tsalta, Madatian, Schubert, Xia, Hardesty, Deng, and Seymour.

Wrote or contributed to the writing of the manuscript: Tsalta, Madatian, Schubert, Xia, Hardesty, Deng, and Gorycki.

References

Allan GA, Gedge JI, Nedderman AN, Roffey SJ, Small HF, and Webster R (2006) Pharmacokinetics and metabolism of UK-383,367 in rats and dogs: a rationale of long-lived plasma radioactivity. *Xenobiotica* **36:**399–418.

Bailey MJ and Dickinson RG (1996) Chemical and immunochemical comparison of protein adduct formation of four carboxylate drugs in rat liver and plasma. *Chem Res Toxicol* **9:**659–666.

Bateman KP, Trimble L, Chauret N, Silva J, Day S, Macdonald D, Dube D, Gallant M, Mastracchio A, Perrier H, et al. (2006) Interspecies in vitro metabolism of the phosphodiesterase-4 (PDE4) inhibitor L-454,560. *J Mass Spectrom* **41:**771–780.

Davies B and Morris T (1993) Physiological parameters in laboratory animals and humans. *Pharm Res* **10:**1093–1095.

Eling TE, Wilson AG, Chaudhari A, and Anderson MW (1977) Covalent binding of an intermediate(s) in prostaglandin biosynthesis to guinea pig lung microsomal protein. *Life Sci* **21:**245–251.

Evans DC, Watt AP, Nicoll-Griffith DA, and Baillie TA (2004) Drug-protein adducts: an industrial perspective on minimizing the potential for drug bioactivation in drug discovery and development. *Chem Res Toxicol* **17:**3–16.

Fuccella LM, Goldaniga G, Lovisolo P, Maggi E, Musatti L, Mandelli V, and Sirtori CR (1980) Inhibition of lipolysis by nicotinic acid and by acipimox.*Clin Pharmacol Ther* **28:**790–795.

Grundy SM, Mok HY, Zech L, and Berman M (1981) Influence of nicotinic acid on metabolism of cholesterol and triglycerides in man. *J Lipid Res* **22:**24–36.

Kalgutkar AS and Soglia JR (2005) Minimising the potential for metabolic activation in drug discovery. *Expert Opin Drug Metab Toxicol* **1:**91–142.

Karpe F and Frayn KN (2004) The nicotinic acid receptor—a new mechanism for an old drug. *Lancet* **363:**1892–1894.

Lan SJ, Weliky I, and Schreiber EC (1973) Metabolic studies with trans-5-amino-3-[2-(5-nitro-2-furyl)vinyl]-1,2,4-[5-^{14}C]oxadiazole (SQ 18,506): 1. Reductive cleavage of the 1,2,4-oxadiazole ring. *Xenobiotica* **3:**97–102.

Pampori NA and Shapiro BH (1996) Feminization of hepatic cytochrome P450s by nominal levels of growth hormone in the feminine plasma profile. *Mol Pharmacol* **50:**1148–1156.

Paoloni L and Cignitti M (1968) Electronic structure and chemical properties of 1,2,4-oxadiazole, bis-1,2,4-oxadiazoles and other derivatives. *Tetrahedron* **24:**485–489.

Peters L, Frohlich R, Boyd ASF, and Kraft A (2001) Tetrazole binding to amidine bases. *Fifth International Electronic Conference on Synthetic Organic Chemistry (ECSOC-5)*, pp 1–10; 2001 Sept 1–30; Electronic Conference. International Electronic Conference on Synthetic Organic Chemistry (ECSOC), http://www.mdpi.net/ecsoc-5/.

Peters T Jr (1962) The biosynthesis of rat serum albumin. III. Amino acid composition of rat albumin. *J Biol Chem* **237:**2182–2183.

Robertson GR, Farrell GC, and Liddle C (1998) Sexually dimorphic expression of rat CYP3A9 and CYP3A18 genes is regulated by growth hormone. *Biochem Biophys Res Commun* **242:**57–60.

Saadane A, Neveux N, Feldmann G, Lardeux B, and Bleiberg-Daniel F (1996) Inhibition of liver RNA breakdown during acute inflammation in the rat. *Biochem J* **317:**907–912.

Skett P (1988) Biochemical basis of sex differences in drug metabolism. *Pharmacol Ther* **38:**269–304.

Skonberg C, Olsen J, Madsen KG, Hansen SH, and Grillo MP (2008) Metabolic activation of carboxylic acids. *Expert Opin Drug Metab Toxicol* **4:**425–438.

Speed W, Parton AH, Martin IJ, and Howard MR (1994) The use of liquid chromatography/thermospray mass spectrometry with online ultraviolet diode array and radiochemical detection: characterization of the putative metabolites of U-78875 in female rat feces. *Biol Mass Spectrom* **23:**1–5.

Tunaru S, Kero J, Schaub A, Wufka C, Blaukat A, Pfeffer K, and Offermanns S (2003) PUMA-G and HM74 are receptors for nicotinic acid and mediate its anti-lipolytic effect. *Nat Med* **9:**352–355.

Tyrkov AG (2001) Acid hydrolysis of 3-aryl-5-trinitromethyl-1,2,4-oxadiazoles. *Russ J Org Chem* **37:**1353–1354.

Ulrich RG, Bacon JA, Brass EP, Cramer CT, Petrella DK, and Sun EL (2001) Metabolic, idiosyncratic toxicity of drugs: overview of the hepatic toxicity induced by the anxiolytic, panadiplon. *Chem Biol Interact* **134:**251–270.

Walsh JS, Reese MJ, and Thurmond LM (2002) The metabolic activation of abacavir by human liver cytosol and expressed human alcohol dehydrogenase isozymes. *Chem Biol Interact* **142:**135–154.

Watjen F, Baker R, Engelstoff M, Herbert R, MacLeod A, Knight A, Merchant K, Moseley J, Saunders J, and Swain CJ (1989) Novel benzodiazepine receptor partial agonists: oxadiazolylimidazobenzodiazepines. *J Med Chem* **32:**2282–2291.

Wise A, Foord SM, Fraser NJ, Barnes AA, Elshourbagy N, Eilert M, Ignar DM, Murdock PR, Steplewski K, Green A, et al. (2003) Molecular identification of high and low affinity receptors for nicotinic acid. *J Biol Chem* **278:**9869–9874.

Yabuki M, Shono F, Nakatsuka I, and Yoshitake A (1993) Novel cleavage of the 1,2,4-oxadiazole ring in rat metabolism of SM-6586, a dihydropyridine calcium antagonist. *Drug Metab Dispos* **21:**1167–1169.

Yan Z, Easterwood LM, Maher N, Torres R, Huebert N, and Yost GS (2007) Metabolism and bioactivation of 3-methylindole by human liver microsomes. *Chem Res Toxicol* **20:**140–148.

Zhou L, McKenzie BA, Eccleston ED Jr, Srivastava SP, Chen N, Erickson RR, and Holtzman JL (1996) The covalent binding of [14C]acetaminophen to mouse hepatic microsomal proteins: the specific binding to calreticulin and the two forms of the thiol:protein disulfide oxidoreductases. *Chem Res Toxicol* **9:**1176–1182.

Address correspondence to: Catherine Tsalta, Drug Metabolism and Pharmacokinetics, GlaxoSmithKline, 709 Swedeland Rd., King of Prussia, PA 19406. E-mail: catherine.2.tsalta@gsk.com